

Superconducting junctions with flat bands

P. Virtanen,^{1,*} R. P. S. Penttilä,² P. Törmä,² A. Díez-Carlón,^{3,4} D. K. Efetov,^{3,4} and T. T. Heikkilä¹

¹*Department of Physics and Nanoscience Center, University of Jyväskylä,
P.O. Box 35 (YFL), FI-40014 University of Jyväskylä, Finland*

²*Department of Applied Physics, Aalto University School of Science, FI-00076 Aalto, Finland*

³*Fakultät für Physik, Ludwig-Maximilians-Universität, Schellingstrasse 4, 80799 München, Germany*

⁴*Munich Center for Quantum Science and Technology (MCQST), München, Germany*

(Dated: October 31, 2024)

We analyze the properties of flat-band superconductor junctions that behave differently from ordinary junctions containing only metals with Fermi surfaces. In particular, we show how in the tunneling limit the critical Josephson current between flat-band superconductors is inversely proportional to the pair potential, how the quantum geometric contribution to the supercurrent contributes even in the normal state of a flat-band weak link, and how Andreev reflection is strongly affected by the presence of bound states. Our results are relevant for analyzing the superconducting properties of junctions involving magic-angle twisted bilayer graphene as well as other electronic systems with flat bands.

Most of our knowledge of the properties of superconducting junctions relies on an expansion of the electronic dispersion around the Fermi energy of the electrodes [1–7]. This expansion is often coined *Andreev approximation* to indicate its use in describing the Andreev reflection that is at the heart of generating essentially all relevant effects encountered on those junctions: the proximity effect and the supercurrent, the excess current and the multiple Andreev reflections. Since the Andreev approximation relies on the presence of the Fermi surface, it completely fails for systems that lack it, such as systems containing flat electronic bands. Flat bands are promising for increasing the critical temperature [8] and providing unconventional superconductivity [9] with quantum geometric effects [10], therefore the behavior of superconducting junctions in the flat band limit has become an important open question.

In this Letter, we study how the flat-band nature of the bands modifies the superconducting transport properties of superconducting junctions. The most relevant changes are due to the localization of the energy window relevant to the transport properties and the possibility of supercurrent even in the presence of frozen quasiparticle transport [11]. The latter arises in the case of non-trivial quantum geometry of the flat-band eigenfunctions [12]. Moreover, as the electronic states in flat band systems are inherently localized, many transport properties can be linked to the coupling between bound states. In contrast, in ordinary junctions such bound-state corrections can often be neglected. We illustrate these effects with three results: (i) The critical current of a tunnel junction between flat-band superconductors is inversely proportional to the pair potential, in contrast to the linear dependence in ordinary junctions. (ii) Supercurrent through a flat-band weak link depends crucially on the strength of interactions inside that weak link. Finally, (iii) Andreev reflection from a flat-band superconductor depends on surface bound-state contributions that also

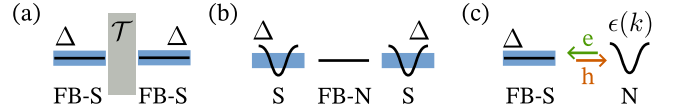


FIG. 1. Junctions between flat-band and dispersive superconductors (with order parameter Δ) and normal-state systems. (a) Superconducting flat-band (FB-S) tunnel junction. (b) Normal flat-band (FB-N) system between superconductors (S). (c) Andreev reflection in flat-band superconductor / normal metal (N) junction.

affect the excess current across the junction. The limit of an exact flat band is a useful idealization. Using example models, we discuss how this limit emerges for the above three properties as a dispersive band becomes flatter. We also identify the relevant limiting scales describing the crossover between ordinary and flat bands.

Tunnel junctions. First, we show that the presence of flat bands can already be identified from the parameter dependence of the critical current in tunnel junctions [see Fig. 1(a)]. The Ambegaokar–Baratoff formula for the Josephson current through two superconductors connected with a simple tunnel junction is the simplest description of such junctions. For two single-band superconductors with equal amplitude superconducting gaps, the zero-voltage Josephson current is given by [5, 13]

$$I_s = \sin(\phi) I_c = \sin(\phi) \frac{4e|\mathcal{T}|^2}{\hbar} k_B T \sum_{i\omega} \sum_{\mathbf{k}\mathbf{p}} F_{\mathbf{k},i\omega}^\dagger F_{\mathbf{p},i\omega'}, \quad (1)$$

where ϕ is the phase difference between the superconducting gaps, I_c is the critical current, \mathcal{T} is the tunneling amplitude, e is the charge of electrons, T is the temperature, k_B the Boltzmann constant, and $F_{\mathbf{k},i\omega} = \frac{\Delta}{\varepsilon_{\mathbf{k}}^2 + \Delta^2 + \omega^2}$ denotes the anomalous Bardeen-Cooper-Schrieffer (BCS) Green’s function. Here, ω is the Matsubara frequency, and Δ is the absolute value of the superconducting gap.

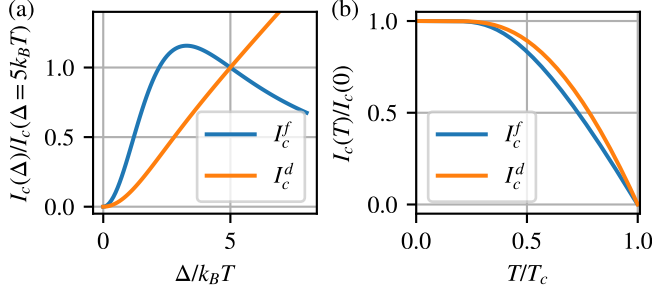


FIG. 2. (a) The flat-band and dispersive Josephson currents as a function of $\Delta/(k_B T)$. (b) The flat-band and dispersive Josephson currents as a function of temperature. The superconducting gap $\Delta(T)$ is solved self-consistently with BCS theory.

The momentum summed Green's functions are different for the regular quadratic dispersion $\varepsilon_{\mathbf{k}}^d = \hbar^2 \mathbf{k}^2 / 2m - \mu$, where μ is the chemical potential, and a flat dispersion $\varepsilon_{\mathbf{k}}^f = 0$:

$$\sum_{\mathbf{k}} F_{\mathbf{k},i\omega}^d = \nu_F \pi \frac{\Delta}{\sqrt{\omega^2 + \Delta^2}}, \quad \sum_{\mathbf{k}} F_{\mathbf{k},i\omega}^f = \frac{\Delta}{\omega^2 + \Delta^2}, \quad (2)$$

where ν_F is the normal-state Fermi-level density of states of the dispersive leads (with units 1/energy). Here, we consider a completely flat band in the whole Brillouin zone. The critical Josephson currents are given by

$$I_c^d = I_{c0}^d \tanh \tilde{\Delta}, \quad I_{c0}^d = 2e |\mathcal{T}|^2 \pi^2 \nu_F^2 \Delta / \hbar \quad (3)$$

$$I_c^{fb} = I_{c0}^{fb} \left[\tanh \tilde{\Delta} - \tilde{\Delta} \operatorname{sech}^2 \tilde{\Delta} \right], \quad I_{c0}^{fb} = \frac{e |\mathcal{T}|^2}{\hbar \Delta} \quad (4)$$

for the dispersive and flat-band cases, respectively. Here $\tilde{\Delta} = \Delta / (2k_B T)$. A notable qualitative difference is the dependence of the zero-temperature critical current on Δ : in the ordinary case I_c is linearly proportional to Δ , whereas, for a flat band, it is inversely proportional to it, up to $\Delta \sim k_B T$ as shown in Fig. 2. The tunneling over the insulating barrier is mediated by virtual pair breaking with probability $|\mathcal{T}|^2 / \Delta$, which explains the $I_{c0}^{fb} \propto 1/\Delta$ behavior in a flat band where all electrons participate in pairing at any value of Δ . In the dispersive case, the fraction of pairs increases with increasing Δ on both sides of the junction, leading to $I_{c0}^d \propto \Delta^2 / \Delta = \Delta$. In the case of weakly dispersive bands with bandwidth J , the relative correction to Eq. (4) is proportional to J^2 / Δ^2 [14], and hence we expect Eq. (4) to hold for $J \ll \Delta$.

Another way to give an intuitive understanding of the FB tunneling current is to consider the coupling of localized states a and b , representing the flat bands, on opposite sides of the tunnel junction. The simplest description in the spin-degenerate case is the Hamiltonian $H = t a_{\uparrow}^{\dagger} b_{\uparrow} + t a_{\downarrow}^{\dagger} b_{\downarrow} + \Delta a_{\uparrow}^{\dagger} a_{\downarrow}^{\dagger} + \Delta e^{i\varphi} b_{\uparrow}^{\dagger} b_{\downarrow}^{\dagger} + \text{h.c.}$ where t is the tunnelling amplitude. It has two Andreev bound

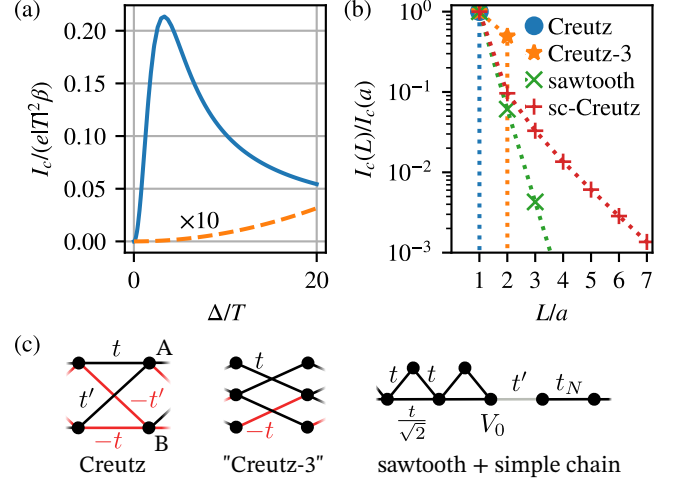


FIG. 3. (a) Dependence of the supercurrent in a flat-band tunnel junction on the interface coupling in the Creutz ladder. Solid: tunneling only between A-sites. Dashed: tunnel hoppings \propto bulk hoppings. Here $\beta = 1/(k_B T)$. (b) S/N/S junction scaling of the supercurrent vs. length of N , for different lattice types. Here “sc-Creutz” is the Creutz ladder with attractive interaction in the N-region, see Fig. 1(b). (c) 1D lattices with flat bands, with hoppings indicated. For the sawtooth ladder, the connection to the simple chain with an edge potential V_0 is illustrated.

states, $\varepsilon_{\pm} = \sqrt{|\Delta|^2 + |t|^2 \pm 2|t\Delta| \sin(\varphi/2)}$ [15]. The supercurrent flowing between the two superconductors is then $I_S(\varphi) = -\frac{2e}{\hbar} N \sum_{\pm} \frac{\partial \varepsilon_{\pm}}{\partial \varphi} \tanh \frac{\varepsilon_{\pm}}{2k_B T}$, where N is the total number of states participating in tunneling [14]. For $t \rightarrow 0$, this reduces to Eq. (4) with $N|t|^2 = |\mathcal{T}|^2 / (2\pi)$. The $1/\Delta$ divergence of the supercurrent at $\Delta \sim k_B T \rightarrow 0$ is cut off at $\Delta \simeq |t|$, where the critical current saturates to $I_c^{fb} \sim \frac{e\Delta}{\hbar} N$. This result also coincides with that in a point contact between flat-band superconductors.

Lattice models. Further insight into the generic nature of the AB results can be obtained by studying lattice models that host flat bands. For simplicity, we concentrate on tight-binding models with finite-range hopping. In them, the physics remains very similar to above, but gains new ingredients: (i) sublattice structure: except for models with trivial insulating flat bands, the unit cell hosts more than one site; (ii) the difference between the boundary and bulk, that is, the presence of Andreev and edge bound states in the lattice.

Accounting for edge effects and sublattice structure, Eq. (1) generalizes to [14, 16]

$$I_S = iT \sum_{\omega_n} \operatorname{tr}(G_{LR} J \tau_3 - G_{RL} J^{\dagger} \tau_3), \quad (5)$$

where $J = J_0 e^{-i\varphi \tau_3 / 2}$ is the tunnel hopping including the phase difference, $G_{LR/RL}$ are elements of the full Green's functions connecting the two sides, and τ_3 is a Pauli matrix in the Nambu space.

In flat bands relying on destructive interference of tunneling from specific orbitals of the unit cell, the supercurrent is sensitive to the details of the tunnel interface. A particular example is tunnel hoppings proportional to the bulk hopping matrix between unit cells, which generally in 1D lattices results in a major cancellation of the leading contribution to the supercurrent found in the AB result. This is illustrated in Fig. 3(a) for the Creutz ladder (Fig. 3(c)). [17] The flat-band peak of Eq. (4) is visible in the case where the tunneling matrix is different from the bulk hopping matrix, whereas in the opposite case, the critical current resembles the ordinary result. This occurs also for other flat-band lattices, as the flat-band pole in the edge Green's function has a sublattice structure orthogonal to the bulk hopping [14].

Superconducting-normal junctions. In junctions where the tunneling weak link is replaced by an extended normal-state (N) layer, generally, the proximity effect and the magnitude of the supercurrent decays as the junction length increases [18, 19]. The spatial extent of the proximity effect can be characterized with the pair correlation function $\Pi(x, x')$ [20], which describes the propagation of a pair of electrons from x to x' . Here, $x = (m, \alpha)$ specifies both unit cell position m and orbital α indices. For a weak proximity effect, it can be written as $\Pi_{\alpha\alpha'}(m, m') = T \sum_{\omega_n} G_{\alpha\alpha'}(m - m', \omega_n) G_{\alpha\alpha'}(m - m', -\omega_n)$, where G is a normal Green's function.

We can make a simple argument to estimate the spatial behavior, in 1D and quasi-1D tight-binding models with finite range hopping, along the lines of Ref. [21]. In these models, the Bloch Hamiltonian $H(k) = \sum_{j=-M}^M H_j e^{ijka}$ is a Laurent polynomial in e^{ika} of order M (range of hopping). Here a is the lattice constant. From Cramer's rule, it then follows that the bulk Green's function $G(k, \omega) = [i\omega - H(k)]^{-1}$ can be written as

$$G(k, \omega) = \frac{\sum_{j=-(N-1)M}^{(N-1)M} e^{ijka} P_{\omega, j}}{\prod_p [i\omega - \epsilon_p(k)]}, \quad (6)$$

where $\epsilon_p(k)$ are the band dispersions of the N-material for bands p , and the numerator is a matrix Laurent polynomial of order $\leq (N-1)M$, which depends on the number N of orbitals per unit cell. Taking the inverse Fourier transform, in real space we find

$$G(m, \omega) = \sum_{j=-(N-1)M}^{(N-1)M} P_{\omega, j} f_{\omega}(m - j), \quad (7)$$

$$f_{\omega}(j) = \int_{-\pi/a}^{\pi/a} \frac{dk a e^{-ijk a}}{2\pi \prod_p [i\omega - \epsilon_p(k)]}. \quad (8)$$

If all bands are exactly flat, then $f(j) \propto \delta_{j0}$, and $G(m, \omega) = 0$ for $|m| > (N-1)M$. Thus, in models with only exact flat bands, compact localized states may carry current up to the distance $\xi_{\max} = (N-1)Ma$, but at

longer distances the correlations vanish. More generally, at distances larger than ξ_{\max} the decay is described by f , which depends *only* on the band dispersions $\epsilon_p(k)$ [22]. For example, with a dispersive band at the Fermi level, this produces the exponential decay on the scale of the ballistic coherence length $\xi \propto \hbar v_F / (2\pi T)$ defined by the Fermi velocity [19]. On the other hand, for a flat band, the long-distance behavior is similar to evanescent decay in insulators: temperature-independent and governed by the energy gap to the nearest dispersive band. A similar estimate for the BdG Hamiltonian implies that in an exact flat band system, also the anomalous Green function vanishes, $F(m - m') = 0$ for $|m - m'| > (N-1)Ma$, as observed in Ref. 23 for specific models.

The short-distance behavior, however, depends not only on band dispersions but also on the band geometry. Define the root mean square (rms) range of the proximity effect as

$$(\delta x)_{\alpha\alpha', \text{rms}}^2 \equiv \frac{\sum_m \Pi_{\alpha\alpha'}(m, 0) a^2 m^2}{2 \sum_m \Pi_{\alpha\alpha'}(m, 0)} = \frac{-\partial_q^2 \Pi_{\alpha\alpha'}(q)|_{q=0}}{2 \Pi_{\alpha\alpha'}(q)|_{q=0}}. \quad (9)$$

Under assumptions of time reversal symmetry and uniform pairing on an isolated flat band, the right-hand side can be related to the Brillouin-zone average of the minimal quantum metric $g(k)$, via $(\delta x)_{\alpha\alpha', \text{rms}}^2 = \int \frac{a dk}{2\pi} g(k)$ [24–26]. A similar relation can also be found for the Cooper pair rms size [27]. However, as the decay of the long-distance tail of Π is governed by the band dispersions, a general relation between the critical current and quantum geometry as suggested in Ref. 28 probably does not exist. An exception is the case of a Gaussian or an exponential Π , where the rms range is given by its decay length.

In Fig. 3(b), we show the dependence of the critical current I_c of an S/N/S junction as a function of the N-region length. Here, N is constructed from the same lattice as S [shown in Fig. 3(c)], but with $\Delta = 0$ on $n = L/a - 1$ lattice sites. The Creutz (taking $t = t'$) and the ‘‘Creutz-3’’ lattices have exact flat bands, and supercurrent vanishes exactly after a finite number of sites. In contrast, the sawtooth lattice has both flat and dispersive bands, which allows for the exponential decay in the critical current as a function of L at a scale determined by the band dispersion.

Interaction-mediated supercurrent. Vanishing of supercurrent due to localization of quasiparticles in the N region may be lifted by a small attractive interaction. With nontrivial quantum geometry, the superfluid weight is nonzero even if bands are exactly flat, allowing for Cooper pair transport [10, 12]. Importantly, we find that in an S/N/S geometry, the interaction strength in N does not need to be large enough to make N an intrinsic superconductor. This component of the SNS supercurrent is often neglected in systems with dispersive bands, but

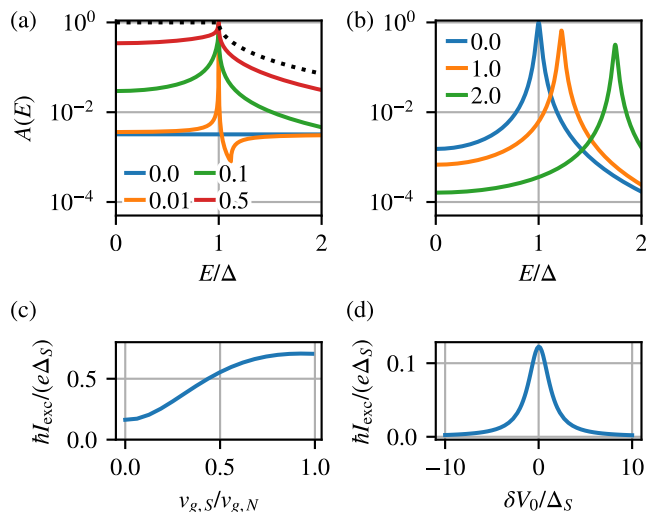


FIG. 4. (a) Andreev reflection probability in a FB-S/N junction from Eq. (13), for different ratios of $v_{g,S}/v_{g,N}$. The dotted line corresponds to the dispersive BTK result for a transparent interface. (b) Resonant Andreev reflection from a sawtooth lattice edge state, for different edge potential offsets δV_0 . (c,d) Corresponding excess current.

in localized flat band systems it is the only long-distance contribution.

In Fig. 3(b), we show a result for the Creutz ladder with small attractive interaction. This is from a mean-field model with local superconducting pair potential $\Delta_i = U\langle c_{i\uparrow}c_{i\downarrow} \rangle$ on each site of the N-region, taking $\mu = -2t$ centered at the lower flat band. For any $U < U_c(T)$ below the interaction required for intrinsic superconductivity, the supercurrent decays exponentially with the system length, $I_c \propto e^{-L/L_g}$ (L_g is defined below). For $U = 0$, there is no supercurrent for $L > a$.

The Ginzburg–Landau (GL) expansion [20] captures the behavior of the interaction-induced component of SNS critical current. Given (quasi-)1D GL free energy density for the N-region,

$$F = \frac{1}{2} \mathcal{A} D(T) |\partial_x \Delta|^2 + A b(T) |\Delta|^2, \quad (10)$$

where \mathcal{A} is the cross-sectional area (3D) or width (2D) of the junction, the interaction-mediated critical current is, in long junctions $L > L_g$,

$$I_{c,\text{int}} \simeq 8 A b(T) \Delta_S^2 L_g e^{-L/L_g}, \quad (11)$$

where $L_g = \sqrt{D(T)/[2b(T)]}$, and Δ_S is the pair potential of the S-leads. The GL expansion assumes $\Delta_S \ll T$. Importantly, the result can also be nonzero if the bands are exactly flat. For the above Creutz ladder model at $\mu = -2t$, $t = t'$ (and assuming the orbitals A and B coincide spatially which makes the quantum metric equal the minimal quantum metric [29, 30]), the expansion gives $D = \frac{\xi_g^2}{4T}$, $b = \frac{2}{U} - \frac{1}{4T}$, $T_c = U/8$. The superfluid weight

D and the decay length scale L_g are proportional to the average of the (minimal) quantum metric tensor $g^{(0)}$ of the flat band,

$$L_g = \xi_g \sqrt{\frac{T_c}{T - T_c}}, \quad \xi_g^2 = a \int_{-\pi/a}^{\pi/a} \frac{dk}{2\pi} g^{(0)}(k). \quad (12)$$

The Creutz ladder GL problem can also be solved without the gradient expansion in Eq. (10) [14], which results in $I_{c,\text{int}} = \frac{\Delta_S^2}{2T} \sqrt{z(z-1)} e^{-L/L_g}$, $L_g = a / \log[2z - 1 + 2\sqrt{z(z-1)}]$ where $z = T/T_c > 1$. Notably, $I_{c,\text{int}}$ does not depend on the normal state resistance unlike the conventional SNS critical current [18, 31], and this could explain anomalous critical current behavior observed in recent experiments on magic-angle twisted bilayer graphene Josephson junctions [32].

Andreev reflection. In the textbook Andreev reflection calculation [33], one matches incoming waves at energy ϵ to evanescent states inside the superconductor at the same energy. For the exact flat band limit, the dispersion of the propagating modes (real \mathbf{k}) is a constant, i.e. $\epsilon(\mathbf{k}) = \epsilon_n$, and analytic continuation implies absence of evanescent modes for any complex \mathbf{k} with $|\mathbf{k}| < \infty$ at energies $\epsilon \neq \epsilon_n$. In lattice models with exact flat bands, solution of the transfer matrix equation shows [14] that the infinitely fast decaying modes become compactly localized, and vanish exactly after a finite number of lattice sites.

The (quasi-)1D tight-binding Andreev scattering problem can be directly solved. For an S/N interface where N consists of 1D chains with hopping t_N at half filling connected to each edge site of S, the backscattering matrix is [14]

$$R = -\frac{1 - gt_N e^{ik_e}}{1 - gt_N e^{-ik_e}}, \quad (13)$$

where $k_e = \arccos(\epsilon/2t_N)$, and g is the Bogoliubov–de Gennes (BdG) surface Green’s function of S. The matrix relates the incoming and outgoing scattering modes in the N lead to each other, $a_{R,\text{out}} = R a_{R,\text{in}}$, and Andreev reflection amplitudes are found in its Nambu off-diagonal components. The backscattering matrix R is unitary at energies where the superconductor does not have propagating modes.

The corresponding Andreev reflection probability for the Creutz ladder as a FB-S [Fig. 1(c)] is illustrated in Fig. 4(a), for $t = t_N = 50\Delta \gg \Delta$, μ tuned at the flat band, and different values of t' allowing to tune the ratio of group velocities $v_{g,S}/v_{g,N}$ on the two sides of the interface. This illustrates the cross-over from a dispersive to an exact flat band on the S-side. The Fermi velocity mismatch between S and N acts similarly to the barrier height in the Blonder-Tinkham-Klapwijk (BTK) model [33]. When approaching the exact flat-band limit, the resonance at $E = \Delta$ gradually disappears and converges to a slowly varying background determined by the

matching of the propagating modes of N to the localized evanescent states of S in its normal state. This picture is also seen for different lattice models.

Flat band systems may additionally host edge states. They are visible as additional poles in g in Eq. (13). If the edge state energies are close to the chemical potential, they provide a resonant Andreev reflection peak in the reflection probability. These resonances generally can be visible in transport properties [11, 34]. In Fig. 4(b) we show the Andreev reflection probability for the sawtooth lattice [cf. Fig. 3(c)], tuning the edge potential $V_0 = -t/\sqrt{2} + \delta V_0$ to align the edge state with the chemical potential $\mu = -t\sqrt{2}$. The resonance peak location is aligned at the edge state, and its width depends on the hybridization of the state with the N-lead; here the coupling was chosen as $t' = t/10$.

Excess current. The integrated Andreev reflection probability $A(\epsilon)$ across energies is experimentally reflected in the excess current [33], $I_{\text{exc}} = e \int_{-\infty}^{\infty} d\epsilon \nu v_g [A(\epsilon, \Delta) - B(\epsilon, \Delta) + B(\epsilon, 0)]$, where B is the normal reflection probability and ν and v_g the density of states and group velocity on the normal side. These are shown in Fig. 4(c,d) corresponding to the cases considered in Fig. 4(a,b). These results demonstrate the strong dependence of the excess current on the matching of the edge state energy with the chemical potential.

Conclusions. We have shown that the characteristics of Josephson junctions are drastically affected by flat bands. The tunneling junction between two flat-band superconductors shows a critical current inversely proportional to the order parameter Δ , opposite to the linear in Δ dependence in the conventional dispersive case. In S/N/S junctions, we observe that interactions in the N-region become increasingly important as the dispersion in N flattens. When N has exactly flat bands, supercurrent is only carried by the interaction component at long distances. Finally, we found that the Andreev reflection and excess current in flat band systems are highly sensitive to the properties of the edge states at the interfaces. These results will be useful in interpreting flat-band experiments, as already indicated in the case of twisted bilayer graphene in Ref. [32], and inspire superconducting devices with new functionalities.

Acknowledgments R.P. acknowledges financial support from the Fortum and Neste Foundation. D.K.E. acknowledges funding from the European Research Council (ERC) under the European Union's Horizon 2020 research and innovation program (grant agreement No. 852927), the German Research Foundation (DFG) under the priority program SPP2244 (project No. 535146365), the EU EIC Pathfinder Grant "FLATS" (grant agreement No. 101099139) and the Keele Foundation as part of the SuperC collaboration. This work was supported by the Research Council of Finland under project numbers 339313 and 354735, by European Union's HORIZON-RIA programme 331 (Grant Agreement No. 101135240

JOGATE), and by Jane and Aatos Erkkö Foundation, Keele Foundation, and Magnus Ehrnrooth Foundation as part of the SuperC collaboration.

* pauli.t.virtanen@jyu.fi

- [1] J. Bardeen, L. N. Cooper, and J. R. Schrieffer, Microscopic Theory of Superconductivity, *Phys. Rev.* **106**, 162 (1957).
- [2] A. F. Andreev, Thermal Conductivity of the Intermediate State in Superconductors, *Sov. Phys. JETP* **19**, 1228 (1964).
- [3] B. D. Josephson, Possible new effects in superconductive tunneling, *Phys. Lett.* **1**, 7 (1962).
- [4] I. Giaever and K. Megerle, Study of superconductors by electron tunneling, *Phys. Rev.* **122**, 1101 (1961).
- [5] V. Ambegaokar, U. Eckern, and G. Schön, Quantum dynamics of tunneling between superconductors, *Phys. Rev. Lett.* **48**, 1745 (1982).
- [6] C. Beenakker, Universal limit of critical-current fluctuations in mesoscopic Josephson junctions, *Phys. Rev. Lett.* **67**, 3836 (1991).
- [7] C. Beenakker, Quantum transport in semiconductor-superconductor microjunctions, *Phys. Rev. B* **46**, 12841 (1992).
- [8] N. B. Kopnin, T. T. Heikkilä, and G. E. Volovik, High-temperature surface superconductivity in topological flat-band systems, *Phys. Rev. B* **83**, 220503 (2011).
- [9] E. Y. Andrei, D. K. Efetov, P. Jarillo-Herrero, A. H. MacDonald, K. F. Mak, T. Senthil, E. Tutuc, A. Yazdani, and A. F. Young, The marvels of moiré materials, *Nat. Rev. Mater.* **6**, 201 (2021).
- [10] P. Törmä, S. Peotta, and B. A. Bernevig, Superconductivity, superfluidity and quantum geometry in twisted multilayer systems, *Nat. Rev. Phys.* **4**, 528 (2022).
- [11] V. A. J. Pyykkönen, S. Peotta, and P. Törmä, Suppression of nonequilibrium quasiparticle transport in flat-band superconductors, *Phys. Rev. Lett.* **130**, 216003 (2023).
- [12] S. Peotta and P. Törmä, Superfluidity in topologically nontrivial flat bands, *Nat. Commun.* **6**, 8944 (2015).
- [13] G. D. Mahan, *Many Particle Physics, Third Edition* (Plenum, New York, 2000).
- [14] See Supplemental Material for details of the derivations.
- [15] Note that the bound state energies differ from the usual point contact result obtained in [6].
- [16] A. Martín-Rodero, F. J. García-Vidal, and A. Levy Yeyati, Microscopic theory of Josephson mesoscopic constrictions, *Phys. Rev. Lett.* **72**, 554 (1994).
- [17] Computer codes used in this manuscript are available at <https://gitlab.jyu.fi/jyucmt/2024-flatband-s-junctions>.
- [18] K. Likharev, Superconducting weak links, *Rev. Mod. Phys.* **51**, 101 (1979).
- [19] A. A. Golubov, M. Y. Kupriyanov, and E. Il'ichev, The current-phase relation in Josephson junctions, *Rev. Mod. Phys.* **76**, 411 (2004).
- [20] A. Larkin and A. Varlamov, *Theory of Fluctuations in Superconductors* (Oxford University Press, 2005).
- [21] L. Chen, T. Mazaheri, A. Seidel, and X. Tang, The impossibility of exactly flat non-trivial Chern bands in

- strictly local periodic tight binding models, *J. Phys. A: Math. Theor.* **47**, 152001 (2014).
- [22] In quasi-1D, dispersions of possible edge states also contribute here.
- [23] M. Thumin and G. Bouzerar, [Correlation functions and characteristic lengthscales in flat band superconductors](#) (2024), [arXiv:2405.06215 \[cond-mat.supr-con\]](#).
- [24] S. A. Chen and K. T. Law, Ginzburg-Landau theory of flat-band superconductors with quantum metric, *Phys. Rev. Lett.* **132**, 026002 (2024).
- [25] J.-X. Hu, S. A. Chen, and K. T. Law, [Anomalous coherence length in superconductors with quantum metric](#) (2024), [arXiv:2308.05686 \[cond-mat.supr-con\]](#).
- [26] M. Iskin, [Coherence length in a dilute flat-band superconductor](#) (2024), [arXiv:2407.08449 \[cond-mat.supr-con\]](#).
- [27] M. Iskin, [Pair size and quantum geometry in a multi-band hubbard model](#) (2024), [arXiv:2409.14921 \[cond-mat.supr-con\]](#).
- [28] Z. C. F. Li, Y. Deng, S. A. Chen, D. K. Efetov, and K. T. Law, [Flat band josephson junctions with quantum metric](#) (2024), [arXiv:2404.09211 \[cond-mat.supr-con\]](#).
- [29] K.-E. Huhtinen, J. Herzog-Arbeitman, A. Chew, B. A. Bernevig, and P. Törmä, Revisiting flat band superconductivity: Dependence on minimal quantum metric and band touchings, *Phys. Rev. B* **106**, 014518 (2022).
- [30] M. Tam and S. Peotta, Geometry-independent superfluid weight in multiorbital lattices from the generalized random phase approximation, *Phys. Rev. Res.* **6**, 013256 (2024).
- [31] P. Dubos, H. Courtois, B. Pannetier, F. Wilhelm, A. Zaikin, and G. Schön, Josephson critical current in a long mesoscopic SNS junction, *Phys. Rev. B* **63**, 064502 (2001).
- [32] A. Díez-Carlón *et al.*, Proximity-induced superconductivity in flat bands of Magic Angle Twisted Bilayer Graphene, in preparation (2024).
- [33] G. E. Blonder, M. Tinkham, and T. M. Klapwijk, Transition from metallic to tunneling regimes in superconducting microconstrictions: Excess current, charge imbalance, and supercurrent conversion, *Phys. Rev. B* **25**, 4515 (1982).
- [34] V. A. J. Pyykkönen, S. Peotta, P. Fabritius, J. Mohan, T. Esslinger, and P. Törmä, Flat-band transport and Josephson effect through a finite-size sawtooth lattice, *Phys. Rev. B* **103**, 144519 (2021).
- [35] D. H. Lee and J. D. Joannopoulos, Simple scheme for surface-band calculations. I, *Phys. Rev. B* **23**, 4988 (1981).
- [36] V. Dwivedi and V. Chua, Of bulk and boundaries: Generalized transfer matrices for tight-binding models, *Phys. Rev. B* **93**, 134304 (2016).
- [37] F. R. Gantmakher, *Theory of Matrices*, Vol. 2 (Chelsea Publishing, 1959).
- [38] K. D. Ikramov, Matrix pencils: Theory, applications, and numerical methods, *J. Math. Sci.* **64**, 783 (1993).
- [39] M. Wimmer, *Quantum transport in nano-structures: From computational concepts to spintronics in graphene and magnetic tunnel junctions*, Ph.D. thesis, Universität Regensburg (2008).
- [40] S. Datta, *Electronic Transport in Mesoscopic Systems* (Cambridge University Press, 1995).

Ambegaokar–Baratoff formula for flat bands

We begin with the tunneling Hamiltonian

$$H = H_R + H_L + H_T = H_R + H_L + \sum_{\mathbf{k}\mathbf{p}\sigma} \mathcal{T}_{\mathbf{k}\mathbf{p}} c_{\mathbf{k}\sigma}^\dagger c_{\mathbf{p}\sigma} + \text{h.c.}, \quad (\text{S1})$$

where H_R and H_L describe the right and the left leads and $\mathcal{T}_{\mathbf{k}\mathbf{p}}$ is the tunneling matrix amplitude from the left lead at momentum \mathbf{k} to the right lead at momentum \mathbf{p} . The tunneling current is given by $I(t) = -e \langle \dot{N}_L(t) \rangle$, where \dot{N}_L is the change in the particle number of the left lead, which is obtained from the commutator between the Hamiltonian and the number operator of the left side, i.e., $\dot{N}_L = i[H, N_L]$. The tunneling current comprises the single-particle current and the Josephson current. In the following, we focus on the Josephson current, which is given by [13]

$$I_s(t) = \frac{2e}{\hbar} \text{Im} \left[e^{-2ietV/\hbar} \Phi(eV) \right], \quad (\text{S2})$$

where $\Phi(eV)$ is the retarded correlation function

$$\Phi(eV) = - \int_{-\infty}^{\infty} dt \Theta(t-t') e^{ieV(t-t')} \langle [A(t), A(t')] \rangle. \quad (\text{S3})$$

Here, $A(t) = \sum_{\mathbf{k}\mathbf{p}\sigma} \mathcal{T}_{\mathbf{k}\mathbf{p}} c_{\mathbf{k}\sigma}^\dagger(t) c_{\mathbf{p}\sigma}(t)$ and $V = (\mu_l - \mu_r)/e$ is the electrical potential difference. The retarded correlation function can be evaluated by defining the Matsubara function $\Phi(i\omega)$ and later making the analytic continuation $i\omega \rightarrow eV + i\delta$ [13].

$$\Phi(i\omega) = - \int_0^\beta d\tau e^{i\omega\tau} \langle T_\tau A(\tau) A(0) \rangle \quad (\text{S4})$$

$$= -2|\mathcal{T}|^2 e^{-i\phi} \sum_{\mathbf{k}\mathbf{p}} k_B T \underbrace{\sum_{i\nu} F_{\mathbf{k},i\nu}^{l\dagger} F_{\mathbf{p},i\nu}^r}_{L_{\mathbf{k}\mathbf{p}}(i\omega)}, \quad (\text{S5})$$

where $F_{\mathbf{k},i\omega}^{l/r} = -\frac{|\Delta|}{(i\omega)^2 - \varepsilon_{\mathbf{k}}^2 - |\Delta|^2}$ are the anomalous Green's functions of the left and right leads, expressed with the absolute values of the superconducting gaps $|\Delta|$, which are assumed to be equal for the leads. Here $\varepsilon_{\mathbf{k}}$ denotes the dispersion of the band and ω the Matsubara frequency. The phase difference between these superconducting gaps has been factored out of the summation, resulting in the term $e^{-i\phi}$. We also suppose that the tunneling matrix elements are independent of the momenta, i.e. $\mathcal{T}_{\mathbf{k}\mathbf{p}} \mathcal{T}_{-\mathbf{k}-\mathbf{p}} = |\mathcal{T}|^2 e^{-i\phi_0}$, where $\phi_0 = 0$ in the presence of time-reversal symmetry in the junction.

We use $L_{\mathbf{k}\mathbf{p}}(i\omega)$ to denote the result of the Matsubara summation of the anomalous Green's functions. Usually, the Matsubara summation should be made before the analytic continuation. However, we consider zero-voltage $V = 0$, where we can do the analytic continuation $i\omega \rightarrow eV + i\delta$ first and obtain

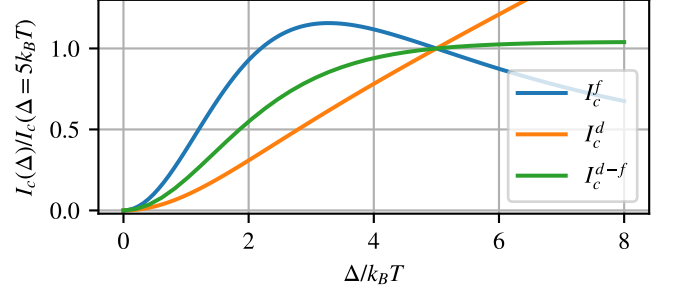


FIG. S1. The Josephson currents as a function of $\Delta/(k_B T)$ for the three possible junctions: dispersive-dispersive, flat-flat, and dispersive-flat.

$$I_s(t) = \frac{4e}{\hbar} \text{Im} \left[-e^{-i\phi} |\mathcal{T}|^2 \sum_{\mathbf{k}\mathbf{p}} L_{\mathbf{k}\mathbf{p}}(eV = 0) \right] \quad (\text{S6})$$

$$= \sin(\phi) \frac{4e}{\hbar} |\mathcal{T}|^2 k_B T \sum_{i\nu} \sum_{\mathbf{k}\mathbf{p}} F_{\mathbf{k},i\nu}^{l\dagger} F_{\mathbf{p},i\nu}^r \quad (\text{S7})$$

$$= \sin(\phi) I_c, \quad (\text{S8})$$

where the current amplitude is given by the critical current I_c . The momentum summed Green's functions are different for the regular quadratic dispersion $\varepsilon_{\mathbf{k}}^d = \hbar^2 \mathbf{k}^2 / 2m - \mu$ and a flat dispersion $\varepsilon_{\mathbf{k}}^f = 0$:

$$\sum_{\mathbf{k}} F_{\mathbf{k},i\omega}^d = \nu_F \pi \frac{|\Delta|}{\sqrt{\omega^2 + |\Delta|^2}}, \quad \sum_{\mathbf{k}} F_{\mathbf{k},i\omega}^f = \frac{|\Delta|}{\omega^2 + |\Delta|^2}, \quad (\text{S9})$$

where ν_F is the normal-state Fermi-level density of states of the dispersive leads. The critical Josephson currents for the flat-flat and dispersive-dispersive cases are obtained by performing the remaining Matsubara summation

$$I_c^d = I_{c0}^d \tanh \tilde{\Delta}, \quad I_{c0}^d = 2e |\mathcal{T}|^2 \pi^2 \nu_F^2 |\Delta| / \hbar \quad (\text{S10})$$

$$I_c^{fb} = I_{c0}^{fb} \left[\tanh \tilde{\Delta} - \tilde{\Delta} \text{sech}^2 \tilde{\Delta} \right], \quad I_{c0}^{fb} = \frac{e |\mathcal{T}|^2}{\hbar |\Delta|} \quad (\text{S11})$$

for the dispersive and flat-band cases, respectively. Here $\tilde{\Delta} = |\Delta| / (2k_B T)$. The current between a dispersive and a flat-band lead is calculated numerically and shown in Fig. S1. For $\Delta \gg k_B T$, I_d is linearly proportional to Δ , and I_f inversely, while I_{d-f} seems to have almost no dependence on Δ .

We can examine the limit of the exact flat band approximation by Taylor expanding the anomalous Green's functions of both leads around zero dispersion $\varepsilon_{\mathbf{k}} = 0$ and taking terms up to second order in $\varepsilon_{\mathbf{k}}$

$$F_{\mathbf{k},i\omega}^{l/r} = \frac{|\Delta|}{\omega^2 + \varepsilon_{\mathbf{k}}^2 + |\Delta|^2} \simeq \frac{|\Delta|}{\omega^2 + |\Delta|^2} \left(1 + \frac{\varepsilon_{\mathbf{k}}^2}{\omega^2 + |\Delta|^2} \right). \quad (\text{S12})$$

Now, the critical current up to second order in $\varepsilon_{\mathbf{k}}$ is given by

$$\frac{I_c \hbar}{4e|\mathcal{T}|^2} \simeq k_B T \sum_{i\omega} \frac{|\Delta|^2}{(\omega^2 + |\Delta|^2)^2} + 2 \frac{E^2 |\Delta|^2}{(\omega^2 + |\Delta|^2)^3}, \quad (\text{S13})$$

where $E^2 = \sum_{\mathbf{k}} \varepsilon_{\mathbf{k}}^2$. The first term produces the flat-band current presented earlier and the second term gives the following second-order correction to the current

$$I_c^{(2)} = I_{c0} \left[\tanh \tilde{\Delta} - \tilde{\Delta} \text{sech}^2 \tilde{\Delta} - \frac{2\tilde{\Delta}^2}{3} \text{sech}^2 \tilde{\Delta} \tanh \tilde{\Delta} \right], \quad (\text{S14})$$

$$I_{c0} = \frac{3e|\mathcal{T}|^2 E^2}{2\hbar|\Delta|^3} \quad (\text{S15})$$

where I_{c0} is the zero temperature current. For a cosine dispersion relation, $\varepsilon_{\mathbf{k}} = \mu - J \sum_{i=x,y,z} \cos(k_i a)$, where J represents the bandwidth, at half-filling ($\mu = 0$) the prefactor is given by $E^2 = \frac{3J^2}{2}$. Thus, at zero temperature, the ratio of the second-order current correction to the exact flat-band current is

$$\frac{I_0^{(2)}}{I_0^f} = \frac{9J^2}{4|\Delta|^2} \quad (\text{S16})$$

In other words, the flat-band expression for the critical supercurrent, Eq. (4) in the main text, is valid when $|\Delta| \gg J$.

The temperature-dependent superconducting gap $\Delta(T)$, used in Fig. 2(b) of the main text, is solved self-consistently with BCS theory. In the dispersive case, the result is the usual BCS superconducting gap, with $\Delta(0) \approx 1.76 k_B T_c$ [1] and in the flat-band case the $\Delta(T)$ is solved from $2/U = \sum_{\mathbf{k}} \tanh(\sqrt{\Delta^2 + \varepsilon_{\mathbf{k}}^2}/2k_B T) / \sqrt{\Delta^2 + \varepsilon_{\mathbf{k}}^2}$, with $\varepsilon_{\mathbf{k}} = 0$, for which $\Delta(0) \approx 2k_B T_c$.

Tunnel junctions on a lattice

The tunneling approximation for the supercurrent between two flat-band superconductors has an unusual feature: the result diverges as $1/\Delta$ when one sets $T \sim \Delta$. Here we derive the simple models used in the main text for understanding the result nonperturbatively.

Consider the BdG tight-binding Hamiltonian of a bilayer system, with weak tunneling T between the layers:

$$H = \begin{pmatrix} H_L & T^\dagger \\ T & H_R \end{pmatrix}, \quad (\text{S17})$$

Consider now a point contact, where the tunneling amplitude matrix element is nonzero only at a single position

$$T_{\mathbf{r}\mathbf{r}'} = t\tau_3 \delta_{\mathbf{r},\mathbf{0}} \delta_{\mathbf{r}',\mathbf{0}}. \quad (\text{S18})$$

Here, \mathbf{r} are unit cell coordinates, and $t = t^*$ is a matrix with a possible time-reversal symmetric orbital structure inside the unit cell. With the usual Fourier definitions, $\psi(\mathbf{k}) = \sum_{\mathbf{r}} e^{i\mathbf{r}\cdot\mathbf{k}} \psi(\mathbf{r}) \equiv \sum_j e^{i\mathbf{r}_j\cdot\mathbf{k}} \psi(\mathbf{r})$ sum over unit cells, and $\psi(\mathbf{r}) = \sum_{\mathbf{k}} e^{-i\mathbf{r}\cdot\mathbf{k}} \psi(\mathbf{k}) \equiv \frac{A_{\text{uc}}}{(2\pi)^d} \int_{\text{BZ}} d^d k e^{-i\mathbf{r}\cdot\mathbf{k}} \psi(\mathbf{k})$, we have $T_{\mathbf{k}\mathbf{k}'} = \sum_{\mathbf{r}\mathbf{r}'} e^{i\mathbf{r}\cdot\mathbf{k} - i\mathbf{r}'\cdot\mathbf{k}'} T_{\mathbf{r}\mathbf{r}'} = t\tau_3$. Here A_{uc} is the area of the unit cell.

We can recall the solution to this problem. [16] The equation $(\varepsilon - H)G = 1$ reads

$$\begin{pmatrix} G_{L0,\mathbf{k}}^{-1} & 0 \\ 0 & G_{R0,\mathbf{k}}^{-1} \end{pmatrix} G_{\mathbf{k},\mathbf{k}'} - \begin{pmatrix} 0 & t^\dagger \tau_3 \\ t\tau_3 & 0 \end{pmatrix} \sum_{\mathbf{q}} G_{\mathbf{q},\mathbf{k}'} = \delta_{\mathbf{k}\mathbf{k}'}, \quad (\text{S19})$$

where $G_{L/R0,\mathbf{k}}^{-1} = i\omega - H_{L/R}(\mathbf{k})$. This results to

$$G_{\mathbf{k},\mathbf{k}'} = \begin{pmatrix} 0 & G_{L0,\mathbf{k}} t^\dagger \tau_3 \\ G_{R0,\mathbf{k}} t\tau_3 & 0 \end{pmatrix} \sum_{\mathbf{q}} G_{\mathbf{q},\mathbf{k}'} + \begin{pmatrix} G_{L0,\mathbf{k}} & 0 \\ 0 & G_{R0,\mathbf{k}} \end{pmatrix} \delta_{\mathbf{k}\mathbf{k}'}. \quad (\text{S20})$$

Summing over \mathbf{k} , and writing $g_{L/R} = \sum_{\mathbf{k}} G_{L/R0,\mathbf{k}}$,

$$\sum_{\mathbf{k}} G_{\mathbf{k},\mathbf{k}'} = \begin{pmatrix} 0 & g_L t^\dagger \tau_3 \\ g_R t\tau_3 & 0 \end{pmatrix} \sum_{\mathbf{k}} G_{\mathbf{k},\mathbf{k}'} + \begin{pmatrix} G_{L0,\mathbf{k}'} & 0 \\ 0 & G_{R0,\mathbf{k}'} \end{pmatrix}. \quad (\text{S21})$$

Hence,

$$G_{\mathbf{r}\mathbf{r}'=\mathbf{0}\mathbf{0}'} = \sum_{\mathbf{k}\mathbf{k}'} G_{\mathbf{k},\mathbf{k}'} = \begin{pmatrix} 1 & -g_L t^\dagger \tau_3 \\ -g_R t\tau_3 & 1 \end{pmatrix}^{-1} \begin{pmatrix} g_L & 0 \\ 0 & g_R \end{pmatrix} \quad (\text{S22})$$

The left/right off-diagonal blocks of this matrix read

$$G_{LR} = (1 - g_L t^\dagger \tau_3 g_R t\tau_3)^{-1} g_L t^\dagger \tau_3 g_R, \quad (\text{S23})$$

$$G_{RL} = g_R t\tau_3 (1 - g_L t^\dagger \tau_3 g_R t\tau_3)^{-1} g_L. \quad (\text{S24})$$

The supercurrent between the layers is obtained by $t \mapsto t e^{i\delta\varphi\tau_3/2}$ and varying the electronic free energy $F = T \sum_{\omega_n} \text{tr}[i\omega_n - H]$ in $\delta\varphi$, which gives the standard formula [16]:

$$I_S = \frac{e}{i\hbar} T \sum_{\omega_n} \text{tr}(G_{LR} t - G_{RL} t^\dagger) \quad (\text{S25})$$

$$= \frac{e}{i\hbar} T \sum_{\omega_n} \text{tr}\{(1 - g_L t^\dagger \tau_3 g_R t\tau_3)^{-1} g_L t^\dagger [\tau_3, g_R] t\} \quad (\text{S26})$$

$$= \frac{-2e}{\hbar} T \sum_{\omega_n} \partial_{\delta\varphi} \ln \det D(\delta\varphi, \omega_n)|_{\delta\varphi=0}, \quad (\text{S27})$$

$$D(\delta\varphi, \omega) = 1 - g_L t^\dagger e^{-i\delta\varphi\tau_3/2} \tau_3 g_R t e^{i\delta\varphi\tau_3/2} \tau_3. \quad (\text{S28})$$

For $t \rightarrow 0$, this reduces to the Ambegaokar-Baratoff formula in the approximation of momentum-independent

tunneling. To find the current for an extended junction area A in the $t \rightarrow 0$ limit, one can multiply the above single-site contribution by A/A_{uc} , the number of unit cells in the junction area. This effectively assumes the junction interface is rough and does not conserve momentum.

In the opposite case of a smooth interface between the layers, $T_{\mathbf{r}\mathbf{r}'} = t\tau_3\delta_{\mathbf{r}\mathbf{r}'}$, one finds Eq. (S26) but with $g_{L/R} \mapsto G_{L/R0,\mathbf{k}}$ and $\sum_{\omega_n} \mapsto (A/A_{\text{uc}})\sum_{\omega_n,\mathbf{k}}$. For a flat band filling the whole Brillouin zone, one has $g_{L/R} = G_{L/R0,\mathbf{k}}$, and both cases give the same supercurrent. In contrast, for dispersive bands whether the interface conserves parallel momentum or not can matter.

With the simple flat-band model of the main text, Eq. (S26) for the single-site current becomes:

$$I_S = \frac{4e}{i\hbar} \sum_{\omega} \frac{T\Delta_S^2 |t|^2 \sin \phi}{\prod_{\pm} (\omega_n^2 + \Delta_S^2 + |t|^2 \pm 2\Delta_S |t| \sin \frac{\phi}{2})}. \quad (\text{S29})$$

The terms $\propto |t|$ in the denominator provide a cutoff for the $1/T$ divergence of the supercurrent.

Evaluating the Matsubara sum gives the supercurrent in the Andreev bound state form:

$$I_S = \frac{e}{2\hbar} \sum_{\pm} \frac{\mp \Delta_S |t| \sin(\varphi) \tanh \frac{\sqrt{\Delta_S^2 + |t|^2 \pm 2\Delta_S |t| \sin \frac{\varphi}{2}}}{2T}}{|\sin \frac{\varphi}{2}| \sqrt{\Delta_S^2 + |t|^2 \pm 2\Delta_S |t| \sin \frac{\varphi}{2}}} \quad (\text{S30})$$

$$= -\frac{2e}{\hbar} \sum_{\pm} \frac{\partial \epsilon_{\pm}}{\partial \varphi} \tanh \frac{\epsilon_{\pm}}{2T}, \quad (\text{S31})$$

$$\epsilon_{\pm} = \sqrt{\Delta_S^2 + |t|^2 \pm 2\Delta_S |t| \sin \frac{\varphi}{2}}. \quad (\text{S32})$$

For $|t| \rightarrow 0$, this approaches the Ambegaokar-Baratoff result.

The energies ϵ_{\pm} are also the eigenenergies of the Hamiltonian

$$H = \begin{pmatrix} 0 & \Delta_S & t & 0 \\ \Delta_S & 0 & 0 & -t \\ t & 0 & 0 & \Delta_S e^{i\varphi} \\ 0 & -t & \Delta_S e^{-i\varphi} & 0 \end{pmatrix}. \quad (\text{S33})$$

In this minimal model, the flat band is thought to be formed by localized quasiparticle states, between which the tunneling occurs. The tunneling is then always a local process, and momentum conservation at the interface does not matter, which is why the extended interface model, the point-contact model, and this two-state model, give equivalent results for the supercurrent per tunneling site.

Note that the above result differs from the usual dispersive superconductor point contact supercurrent, [6] which is generated by an Andreev bound state with energy $\epsilon_A = \Delta \sqrt{1 - \tau \sin^2 \frac{\varphi}{2}}$, where $0 \leq \tau \leq 1$ is a junction

transparency. The transparency is a function of the tunneling amplitudes and the dispersion parameters [16].

For more complex models, the result also depends on which sites in the unit cell the tunneling matrix t connects, as the currents may interfere destructively. For an isolated time-reversal symmetric flat band, Green's function $G = (i\omega - H_{\text{BdG}})^{-1}$ can be approximated by its flat-band part, as other terms are suppressed by the band gaps. Then, in Eq. (S27)

$$g_{L/R} \approx g_{0,L/R} \otimes P_0, \quad P_0 = \sum_{\mathbf{k}} \psi_{\mathbf{k},0} \psi_{\mathbf{k},0}^{\dagger}, \quad (\text{S34})$$

$$g_{0,L/R} = \frac{-1}{\omega^2 + \varepsilon_0^2 + |\tilde{\Delta}|^2} \begin{pmatrix} i\omega + \varepsilon_0 & \tilde{\Delta} \\ \tilde{\Delta}^* & i\omega - \varepsilon_0 \end{pmatrix}, \quad (\text{S35})$$

where ε_0 and $\psi_{\mathbf{k},0}$ are the energy and Bloch functions of the flat band and $\tilde{\Delta}$ its superconducting gap. Then, $\det D = \prod_j \det(1 - \lambda_j g_{0,L} \tau_3 e^{-i\delta\varphi\tau_3/2} g_{0,R} \tau_3 e^{i\delta\varphi\tau_3/2})$, where λ_j are the eigenvalues of $P_0 L t^{\dagger} P_0 R t$. The total supercurrent is then found by summing the single-channel result (S31) over the effective tunnel amplitudes $|t|^2 \mapsto |\lambda_j|$.

Compactly localized evanescent modes

To understand how the S/N Andreev reflection problem [33] discussed in the main text behaves when the superconductor is a flat-band system, and how this is visible in the resulting scattering amplitude formulas, it is useful to first revisit the textbook calculation. Below, we first point out the main physics and then describe the lattice formulation of the scattering problem and its general solution.

Consider an S/N interface with a superconductor at $x < 0$ and a normal metal at $x > 0$. In the textbook Andreev reflection calculation, evanescent modes at $x < 0$ are matched to propagating modes at $x > 0$, which determines the scattering amplitudes.

Assume now the superconductor has an exact flat band with the energy dispersion

$$\epsilon_{\mathbf{k}n} = \epsilon_n = \text{constant}. \quad (\text{S36})$$

Evanescent modes $\psi(\mathbf{r}) \propto e^{\kappa(\epsilon)x}$, or in lattice models $\psi_j \propto e^{\kappa(\epsilon)aj}$ with j the unit cell index, are (unbounded) solutions of the BdG equation at energy ϵ inside the energy gap of S. The wave vectors $\kappa = ik_x$ are determined by the complex roots of $\epsilon_{\mathbf{k}n} = \epsilon$. However, the analytic continuation of a constant to the complex plane is a constant. This implies that the continuum formulation of the problem is somewhat ill-defined: no such modes exist at energies $\epsilon \neq \epsilon_n$, reflecting the zero group velocity and localization of the quasiparticle states in a flat band. Conversely, exactly at $\epsilon = \epsilon_n$, the equation would in principle be solved by any \mathbf{k} , which reflects the existence of a large number of states at the exact flat band energy.

When there is slight dispersion,

$$\epsilon_{\mathbf{k}n} = \epsilon_n + \eta g(\mathbf{k}), \quad (\text{S37})$$

where η is small, in the ‘‘usual’’ case (e.g., analytic g) the equation $\epsilon_{\mathbf{k}n} = \epsilon$ has solutions $\mathbf{k} = g^{-1}(\frac{\epsilon - \epsilon_n}{\eta})$ for almost all ϵ . Also, as $\eta \rightarrow 0$ the evanescent modes would tend toward large $|\mathbf{k}|$, and their decay becomes faster as the band flattens. In the exact flat band limit, the evanescent decay factor $\lambda = e^{\kappa a}$ must then be $\lambda = 0$ (or $\lambda = \infty$ for waves decaying to opposite direction); that is, there are no *finite* solutions the equation $\epsilon_{\mathbf{k}n} = \epsilon$. In lattice models, this however does not imply that evanescent waves inside the flat band drop to zero within one unit cell, as the above only rules out exponential solutions. A possibility that is left is nilpotent decay, where the wave function becomes zero after some number of unit cells.

Consider now a noninteracting (quasi) one-dimensional tight-binding model, with the block structure

$$\hat{H}_{i,j} = \delta_{i-1,j} \hat{J}_j + \delta_{i,j} \hat{K}_j + \delta_{i+1,j} \hat{J}_{j+1}^\dagger. \quad (\text{S38})$$

Here \hat{J} of size $N \times N$ describes the hopping between unit cells with N sites. Choosing the unit cell large enough, all models with finite-range hopping can be brought to this form. Let us first assume \hat{J}_j and \hat{K}_j are independent of j .

The evanescent modes at energy ϵ are local solutions to the equation $(\hat{H} - \epsilon)\psi = 0$. It is convenient to rewrite the problem as a transfer matrix equation [35], defining $\phi_j = (\psi_j; \psi_{j+1})$,

$$A\phi_{j-1} \equiv \begin{pmatrix} J & K - \epsilon \\ 0 & 1 \end{pmatrix} \phi_{j-1} = \begin{pmatrix} 0 & -J^\dagger \\ 1 & 0 \end{pmatrix} \phi_j \equiv B\phi_j. \quad (\text{S39})$$

The transfer matrix equation for the evanescent modes is associated with the generalized eigenproblem for $A - \lambda B$. In the presence of flat bands, the eigenproblem is not necessarily diagonalizable, as the generalized eigenvalues $0, \infty$ may be highly degenerate and do not originate simply from the zero modes of the hopping matrix. Moreover, transfer matrices $T = A^{-1}B$ or $T = B^{-1}A$ are ill-defined; a system with exact flat bands has only generalized eigenvalues $0, \infty$ and the situation cannot be corrected by making basis transformations [36].

Mathematically, the problem is well understood. The structure is best visible by transforming to the Kronecker canonical form [37, 38], $A = U\tilde{A}V^{-1}$, $B = U\tilde{B}V^{-1}$. We consider now evanescent modes and assume ϵ does not coincide with the spectrum of the Hamiltonian. In this case, the eigenproblem is *regular*. Then, \tilde{A} , \tilde{B} are block-diagonal with blocks of size m_k for each generalized eigenvalue λ_k .

We have $\det(\mu A - \lambda B) = \det(\mu^2 J + (K - \epsilon)\mu\lambda + \lambda^2 J^\dagger) = \mu^N \lambda^N \det[H(k = -i \ln \frac{\lambda}{\mu}) - \epsilon]$ which is not identically

zero except possibly at special values of ϵ . Hence, the matrix pencil $A - \lambda B$ is generically regular and its decomposition contains only the Weierstrass part.

Defining $\tilde{\phi}_j = V^{-1}\phi_j$, Eq. (S39) separates to blocks of two types

$$J_{m_k}(\lambda_k)\tilde{\phi}_{j-1}^k = \tilde{\phi}_j^k, \quad \text{or} \quad \tilde{\phi}_{j-1}^k = J_{m_k}(0)\tilde{\phi}_j^k, \quad (\text{S40})$$

where $\tilde{\phi}_j = (\tilde{\phi}_j^1; \tilde{\phi}_j^2; \dots; \tilde{\phi}_j^M)$, $\sum_{k=1}^M m_k = 2N$, and $[J_m(\lambda)]_{ij} = \lambda\delta_{ij} + \delta_{j,i+1}$ are Jordan blocks of size $m \times m$ for the eigenvalues λ_k . Finite eigenvalues have blocks of the first type, and infinite eigenvalues $\lambda = \infty$ produce blocks of the second type. The same eigenvalue may have multiple blocks. The blocks with $|\lambda_k| > 1$ describe modes decaying toward $j \rightarrow -\infty$, $|\lambda_k| < 1$ those decaying for $j \rightarrow +\infty$, and $|\lambda_k| = 1$ the propagating modes except for $m_k > 1$ of those $m_k - 1$ are polynomially growing.

Pure flat-band systems at $\epsilon \neq \epsilon_n$ have only eigenvalues $\lambda_k = 0, \infty$. Indeed, $\det(\mu A - \lambda B) = \mu^N \lambda^N \prod_n (\epsilon_n - \epsilon)$, so both have multiplicity N . Moreover, the coefficient matrix of Eqs. (S40) is nilpotent, $J_m(0)^m = 0$, and therefore these evanescent modes become zero after $m_k \leq N$ lattice sites. This describes how the localized states in the flat band system participate in evanescent transport. If all $m_k = 1$ for a pure flat-band system, then $J = 0$, so nontrivial pure flat-band systems generally have some $m_k > 1$.

Numerically, the Kronecker decomposition is unstable to calculate, and one should instead use the generalized Schur decomposition. Schur decomposition algorithms for solving the quantum transport problem [39] generally work also for the flat-band lattices. Analytically, the Kronecker decomposition however tends to be easier to calculate.

The transition in the wave functions when going from slight dispersion Eq. (S37) to exact flat band Eq. (S36) should be smooth. However, the nontrivial Jordan block structure with $m_k > 1$ is fragile and requires fine-tuning conditions that can exist in exact flat bands, but would not be present in generically perturbed slightly dispersive models. That there is no contradiction is a consequence of the non-Hermiticity of the evanescent mode problem. As the dispersion approaches a flat band with some $m_k > 1$, the eigenvectors (columns of V) of corresponding groups of eigenvalues become increasingly parallel. This enables approaching the nilpotent decay as $\eta \rightarrow 0$ despite $|\mathbf{k}| \rightarrow \infty$, and ensures that the exact flat band limit can give useful insight also into models where the exact flat band condition is lifted by slight dispersion.

Obtaining the normal state Green’s function g from the Kronecker decomposition

In the problems of finding the supercurrent or Andreev reflection amplitude discussed in the main text, the necessary information about a semi-infinite lead is captured

$$B' = \begin{pmatrix} 0 & 0 & 0 & 0 & 0 & 0 & 0 & 0 \\ 0 & 0 & 0 & 0 & -2t & 0 & 0 & 0 \\ 0 & 0 & 0 & 0 & 0 & 0 & 0 & 0 \\ 0 & 0 & 0 & 0 & 0 & 0 & 2t & 0 \\ 1 & 0 & 0 & 0 & 0 & 0 & 0 & 0 \\ 0 & 1 & 0 & 0 & 0 & 0 & 0 & 0 \\ 0 & 0 & 1 & 0 & 0 & 0 & 0 & 0 \\ 0 & 0 & 0 & 1 & 0 & 0 & 0 & 0 \end{pmatrix}, \quad (\text{S51})$$

$$u = \frac{1}{\sqrt{2}} 1_{4 \times 4} \otimes \begin{pmatrix} 1 & 1 \\ 1 & -1 \end{pmatrix}. \quad (\text{S52})$$

The Kronecker decomposition of (A', B') is

$$a' = \begin{pmatrix} 0 & 1 & 0 & 0 & 0 & 0 & 0 & 0 \\ 0 & 0 & 0 & 0 & 0 & 0 & 0 & 0 \\ 0 & 0 & 0 & 1 & 0 & 0 & 0 & 0 \\ 0 & 0 & 0 & 0 & 0 & 0 & 0 & 0 \\ 0 & 0 & 0 & 0 & 1 & 0 & 0 & 0 \\ 0 & 0 & 0 & 0 & 0 & 1 & 0 & 0 \\ 0 & 0 & 0 & 0 & 0 & 0 & 1 & 0 \\ 0 & 0 & 0 & 0 & 0 & 0 & 0 & 1 \end{pmatrix}, \quad (\text{S53})$$

$$b' = \begin{pmatrix} 1 & 0 & 0 & 0 & 0 & 0 & 0 & 0 \\ 0 & 1 & 0 & 0 & 0 & 0 & 0 & 0 \\ 0 & 0 & 1 & 0 & 0 & 0 & 0 & 0 \\ 0 & 0 & 0 & 1 & 0 & 0 & 0 & 0 \\ 0 & 0 & 0 & 0 & 0 & 1 & 0 & 0 \\ 0 & 0 & 0 & 0 & 0 & 0 & 0 & 0 \\ 0 & 0 & 0 & 0 & 0 & 0 & 0 & 1 \\ 0 & 0 & 0 & 0 & 0 & 0 & 0 & 0 \end{pmatrix}. \quad (\text{S54})$$

There are two 2×2 Jordan blocks corresponding to the generalized eigenvalue 0 with degeneracy 4 (sorted first in the decomposition), and similarly for the infinite eigenvalue. The size of these blocks directly determines the compact localization of the evanescent states.

Note that the decomposition is not valid at the flat-band energies, $\epsilon = \pm\sqrt{\Delta^2 + (\mu \pm 2t)^2}$, where the generalized eigenvalue problem is no longer regular. In this case, the decomposition contains non-square blocks that correspond to the compactly localized flat-band eigenstates.

The transformation matrices are (via computer algebra, see `creutz.sage` [17])

$$U' = \begin{pmatrix} 0 & 0 & 0 & 0 & 0 & -\frac{\Delta^2 \epsilon - \epsilon^3 + \Delta^2 \mu - \epsilon^2 \mu + \epsilon \mu^2 + \mu^3 + 4 \epsilon t^2 - 4 \mu t^2}{\Delta^2 - \epsilon^2 + \mu^2} & 0 & \frac{(\Delta^2 - \epsilon^2 + \mu^2 + 4 t^2) \Delta}{\Delta^2 - \epsilon^2 + \mu^2} \\ 0 & -2t & 0 & 0 & -2t & 0 & 0 & 0 \\ 0 & 0 & 0 & 0 & 0 & \frac{(\Delta^2 - \epsilon^2 + \mu^2 + 4 t^2) \Delta}{\Delta^2 - \epsilon^2 + \mu^2} & 0 & -\frac{\Delta^2 \epsilon - \epsilon^3 - \Delta^2 \mu + \epsilon^2 \mu + \epsilon \mu^2 - \mu^3 + 4 \epsilon t^2 + 4 \mu t^2}{\Delta^2 - \epsilon^2 + \mu^2} \\ 0 & 0 & 0 & 2t & 0 & 0 & 2t & 0 \\ 1 & 0 & 0 & 0 & 0 & 1 & 0 & 0 \\ 0 & \frac{\epsilon + \mu}{2t} & 0 & -\frac{\Delta}{2t} & -\frac{2(\epsilon - \mu)t}{\Delta^2 - \epsilon^2 + \mu^2} & 0 & \frac{2\Delta t}{\Delta^2 - \epsilon^2 + \mu^2} & 0 \\ 0 & 0 & 1 & 0 & 0 & 0 & 0 & 1 \\ 0 & \frac{\Delta}{2t} & 0 & -\frac{\epsilon - \mu}{2t} & -\frac{2\Delta t}{\Delta^2 - \epsilon^2 + \mu^2} & 0 & \frac{2(\epsilon + \mu)t}{\Delta^2 - \epsilon^2 + \mu^2} & 0 \end{pmatrix}, \quad (\text{S55})$$

$$V' = \begin{pmatrix} 1 & 0 & 0 & 0 & 0 & 0 & 0 & 0 \\ 0 & \frac{\epsilon + \mu}{2t} & 0 & -\frac{\Delta}{2t} & 0 & -\frac{2(\epsilon - \mu)t}{\Delta^2 - \epsilon^2 + \mu^2} & 0 & \frac{2\Delta t}{\Delta^2 - \epsilon^2 + \mu^2} \\ 0 & 0 & 1 & 0 & 0 & 0 & 0 & 0 \\ 0 & \frac{\Delta}{2t} & 0 & -\frac{\epsilon - \mu}{2t} & 0 & -\frac{2\Delta t}{\Delta^2 - \epsilon^2 + \mu^2} & 0 & \frac{2(\epsilon + \mu)t}{\Delta^2 - \epsilon^2 + \mu^2} \\ 0 & 1 & 0 & 0 & 0 & 1 & 0 & 0 \\ 0 & 0 & 0 & 0 & -\frac{2(\epsilon - \mu)t}{\Delta^2 - \epsilon^2 + \mu^2} & 0 & \frac{2\Delta t}{\Delta^2 - \epsilon^2 + \mu^2} & 0 \\ 0 & 0 & 0 & 1 & 0 & 0 & 0 & 1 \\ 0 & 0 & 0 & 0 & -\frac{2\Delta t}{\Delta^2 - \epsilon^2 + \mu^2} & 0 & \frac{2(\epsilon + \mu)t}{\Delta^2 - \epsilon^2 + \mu^2} & 0 \end{pmatrix}. \quad (\text{S56})$$

The decomposition of (A, B) is (UaV^{-1}, UbV^{-1}) with $a = a'$, $b = b'$, $U = u^\dagger U'$, $V = u^\dagger V'$.

Knowing the decomposition, we can find the surface Green's function g from Eq. (S43). By direct calculation, we find a simple result

$$g = (\epsilon - K - \Sigma)^{-1}, \quad (\text{S57})$$

$$\Sigma = \frac{2t^2}{\Delta^2 + \mu^2 - \epsilon^2} \begin{pmatrix} \mu - \epsilon & \Delta \\ \Delta & -\mu - \epsilon \end{pmatrix} \otimes \begin{pmatrix} 1 & 1 \\ 1 & 1 \end{pmatrix}, \quad (\text{S58})$$

for the right edge of the semi-infinite chain. The pole in Σ is from the edge state of the Creutz ladder.

The surface Green's function itself then is

$$\begin{aligned} g_\gamma &= \frac{1}{2} \frac{1}{\Delta^2 + \mu^2 - \epsilon^2} \begin{pmatrix} \mu - \epsilon & -\Delta \\ -\Delta & -\mu - \epsilon \end{pmatrix} \otimes \begin{pmatrix} 1 & -\gamma \\ -\gamma & 1 \end{pmatrix} \\ &+ \frac{1}{4} \sum_{\alpha=\pm} \frac{1}{\Delta^2 + (\mu - 2\alpha t)^2 - \epsilon^2} \\ &\times \begin{pmatrix} \mu - 2\alpha t - \epsilon & -\Delta \\ -\Delta & -\mu + 2\alpha t - \epsilon \end{pmatrix} \otimes \begin{pmatrix} 1 & \gamma \\ \gamma & 1 \end{pmatrix}, \end{aligned} \quad (\text{S59})$$

where $\gamma = +1$ for the right edge of a semi-infinite chain and $\gamma = -1$ for the left edge, which can be found from a similar calculation. Here, $\alpha = \pm$ is the band index. The first line is the edge state contribution and the remainder is that of the flat bands at $\epsilon = \pm 2t$.

The suppression of tunneling current shown in Fig. 3 of the main text is also apparent here:

$$I_c \propto \text{tr } f_R J_T f_L J_T^\dagger. \quad (\text{S60})$$

Here f_L and f_R are the anomalous Green's functions on the left/right sides of the tunnel junction, and J_T is the tunneling amplitude matrix. If $J_T \propto J$, then $J_T f_L J_T^\dagger \propto \Sigma$. Since Σ contains only the pole contribution from the edge state which is separated in energy from the flat band by t , the current is suppressed by a factor of $(\Delta/t)^2$ when the chemical potential $\mu = \pm 2t$ is aligned with the flat band.

This behavior originates from the recurrence relation $(\epsilon - K - JgJ^\dagger)g = 1$ of the surface Green's function, and appears fairly generic across quasi-1D exact flat-band lattice models. Namely, separating a flat-band pole part $g = g_{\text{pole}} + g_{\text{smooth}}$, $g_{\text{pole}} = A_{\text{pole}}/(\epsilon - \epsilon_{FB})$, the relation becomes

$$\begin{aligned} Jg_{\text{pole}}J^\dagger g_{\text{pole}} &= (\epsilon - K)g - 1 - Jg_{\text{smooth}}J^\dagger g_{\text{smooth}} \\ &- Jg_{\text{smooth}}J^\dagger g_{\text{pole}} - Jg_{\text{pole}}J^\dagger g_{\text{smooth}}, \end{aligned} \quad (\text{S61})$$

where the right-hand side contains at most one g_{pole} in each term. Collecting terms in different orders in $\propto (\epsilon - \epsilon_{FB})^{-1}$ in the limit $\epsilon \rightarrow \epsilon_{FB}$ one finds that $JA_{\text{pole}}J^\dagger A_{\text{pole}} = 0$. This then can lead to cancellations in tunneling amplitudes.

Using the above results for g in the expression for the backscattering matrix R produces the results show in Fig. 4(a) of the main text.

Interaction-mediated current

We now calculate the critical current in the case the N-material has effective attractive interactions of strength U between the electrons, using a Ginzburg-Landau approach. The Ginzburg-Landau expansion [20] can be found by considering the mean-field free energy of electrons, where a mean field Δ describes the attractive interactions, and expanding in small Δ , namely,

$$F = \sum_x \frac{|\Delta(x)|^2}{U} - T \sum_\omega \text{tr} \ln[i\omega - H] \quad (\text{S62})$$

$$\simeq \sum_{xx'} V(x, x') \Delta(x)^* \Delta(x'). \quad (\text{S63})$$

Often the Ginzburg-Landau theory is done in gradient expansion, so that

$$F = \sum_x [\mathcal{A} \frac{D}{2} |\partial_x \Delta(x)|^2 + \mathcal{A} b |\Delta(x)|^2] \quad (\text{S64})$$

$$V(x, x') = [-\mathcal{A} \frac{D}{2} \partial_x^2 + \mathcal{A} b] \delta(x - x'). \quad (\text{S65})$$

Above, we considered a quasi-1D problem, i.e., $\Delta(\mathbf{x}) = \Delta(x)$.

Consider then a situation where $\Delta(x = 0)$ is fixed, and other values of Δ are chosen such that F is minimized:

$$\sum_{x'} 2V(x, x') \Delta(x') = z \delta(x) \quad (\text{S66})$$

$$\Delta(x) = \frac{z}{2} V^{-1}(x, 0), \quad z = \frac{2\Delta(0)}{V^{-1}(0, 0)}, \quad (\text{S67})$$

where the inverse V^{-1} is the quasi-1D Ginzburg-Landau propagator.

For a long SNS junction, the supercurrent is proportional to the overlap of the tails of Δ from the S-leads:

$$\Delta(x) \simeq e^{-i\varphi/2} \frac{\Delta_L V^{-1}(x, 0)}{V^{-1}(0, 0)} + e^{i\varphi/2} \frac{\Delta_R V^{-1}(x, L)}{V^{-1}(0, 0)}, \quad (\text{S68})$$

$$F \simeq \text{const.} + \cos(\varphi) \frac{\hbar}{2e} I_{c, \text{int}}, \quad (\text{S69})$$

$$I_{c, \text{int}} \simeq \frac{4e}{\hbar} \frac{\Delta_L \Delta_R}{|V^{-1}(0, 0)|^2} V^{-1}(0, L). \quad (\text{S70})$$

In the gradient expansion, we have

$$V(x, x') = [-\mathcal{A} \frac{D}{2} \partial_x^2 + \mathcal{A} b] \delta(x - x'), \quad (\text{S71})$$

$$V^{-1}(x, x') = \frac{Lg}{\mathcal{A}D} e^{-|x-x'|/Lg}, \quad (\text{S72})$$

$$I_c = 8\mathcal{A}b\Delta_L \Delta_R Lg e^{-L/Lg}, \quad (\text{S73})$$

and $Lg = \sqrt{D/(2b)}$.

Interactions in a Creutz-ladder SNS junction

As an example, we show how the interaction-mediated current appears in the Creutz-ladder. The interacting 1D Creutz-ladder flat-band model is

$$H_0(k) = 2t \begin{pmatrix} \cos(ka) & -i \sin(ka) \\ i \sin(ka) & -\cos(ka) \end{pmatrix} \quad (\text{S74})$$

$$= 2t V_k \sigma_z V_k^\dagger, \quad (\text{S75})$$

$$V_k = \frac{1}{2} \begin{pmatrix} e^{-ika} + 1 & e^{-ika} - 1 \\ e^{-ika} - 1 & e^{-ika} + 1 \end{pmatrix} \quad (\text{S76})$$

$$= \begin{pmatrix} u_k & v_k \end{pmatrix}, \quad (\text{S77})$$

$$H_{\text{BdG}}(n, n') = \begin{pmatrix} H_0(n, n') - \mu & \Delta_n \delta_{nn'} \\ \Delta_n^* \delta_{nn'} & -H_0(n, n') + \mu \end{pmatrix}. \quad (\text{S78})$$

Here, n is the unit cell index, $\sigma_z = \text{diag}(1, -1)$ in the band indices, and a is the distance between unit cells. We have assumed that the positions of the orbitals A and B are at the same location, which makes the quantum metric of this system equal to the minimal quantum metric [29, 30]. With such a choice, any spatially dependent phase factors of the order parameter must be the same for the two orbitals; this justifies the assumption in Eq. (S78) that the order parameters of the two orbitals have the same amplitude and phase. Fourier transforms are as $f_k = \sum_n e^{ikan} f_n$, $f_n = \sum_k e^{-ikan} f_k$, $\sum_k \equiv \int_{-\pi/a}^{\pi/a} \frac{adk}{2\pi}$.

The Ginzburg–Landau expansion of the mean-field free energy then is,

$$F = \sum_{nn'} V(n, n') \Delta(n) \Delta(n'), \quad (\text{S79})$$

$$V(n, n') = \frac{2}{U} \delta_{nn'} - \Pi(n, n'). \quad (\text{S80})$$

Here U is the interaction energy.

The electronic part is

$$\Pi(n, n') = T \sum_{\omega} \text{tr} \{ G_0(n' - n) \bar{G}_0(n - n') \}, \quad (\text{S81})$$

where $G_0 = [i\omega - H_0 + \mu]^{-1}$, $\bar{G}_0 = [i\omega + H_0 - \mu]^{-1}$. This gives

$$\begin{aligned} \Pi(n, n') &= \sum_{kk'} e^{-i(k-k')(n-n')a} \sum_{\alpha\alpha'=\pm} \quad (\text{S82}) \\ &\times \text{tr} V_k \frac{1 + \alpha\sigma_z}{2} V_k^\dagger V_{k'} \frac{1 + \alpha'\sigma_z}{2} V_{k'}^\dagger \\ &\times T \sum_{\omega} \frac{1}{(i\omega - 2t\alpha + \mu)(i\omega + 2t\alpha' - \mu)}. \end{aligned}$$

Let us now set $\mu = -2t$, and restrict to the lower flat band $\alpha = \alpha' = -1$, dropping other terms. The neglected parts are small in $T/\mu \ll 1$.

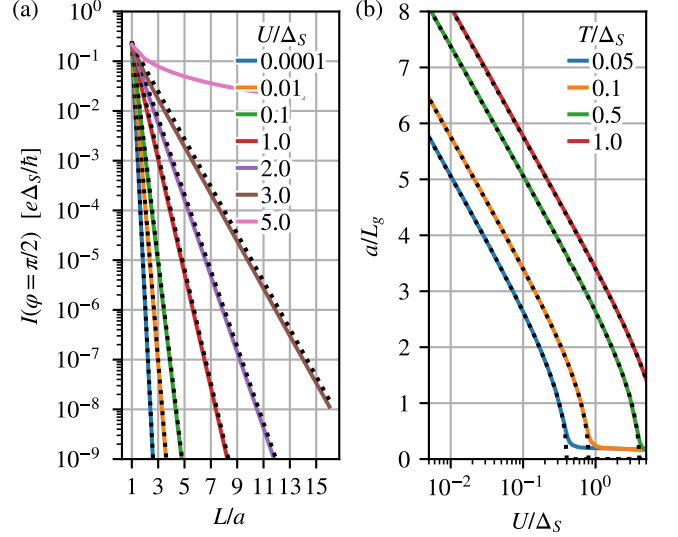


FIG. S2. (a) Supercurrent in S/Creutz-N/S junction vs. length, for different interaction strengths, at temperature $T = \Delta_S/2$. The chemical potential $\mu = -2t$ is at a flat band, and $t = 50\Delta_S$. The critical interaction strength is $U_c = 4\Delta_S$. Solid lines: numerical self-consistent BdG calculation. Black dotted: Eq. (S89). (b) Supercurrent decay length L_g , $I_s \propto e^{-L/L_g}$, vs. interaction strength at different temperatures. Solid lines: the fitted slope of the numerically computed $-\ln I_s(L)$ at large n . Black dotted: Eq. (S88).

Then, taking the Fourier transform

$$\Pi(q) = \frac{1}{4T} \sum_k |v_k^\dagger v_{k-q}|^2, \quad (\text{S83})$$

where $\sum_{\omega} \frac{T}{\omega^2} = 1/(4T)$. For small q , this is directly related to the (minimal) quantum metric,

$$\Pi(q) \simeq \frac{1}{4T} - \frac{1}{4T} \xi_g^2 q^2, \quad \xi_g^2 = \int_{-\pi/a}^{\pi/a} \frac{adk}{2\pi} g(k). \quad (\text{S84})$$

From the above, this is a general feature of flat-band models. [24] Note that for our choice of orbital positions, the quantum metric of the system is automatically the minimal quantum metric. For arbitrary orbital positions, one should do this calculation by considering the orbital positions explicitly, to obtain the dependence on the minimal quantum metric as in Ref. [25].

The Fourier-transformed Ginzburg-Landau propagator is then

$$V^{-1}(q) = \frac{1}{\frac{2}{U} - \Pi(q)} \simeq \frac{4T}{\frac{8T}{U} - 1 + \xi_g^2 q^2}. \quad (\text{S85})$$

The mean-field superconducting transition is at $T_c = U/8$. The quadratic expansion in q implies $V^{-1}(x) \propto e^{-x/L_g}$, where $L_g = \xi_g \sqrt{T_c/(T - T_c)}$.

Since v_k has a very simple form in the Creutz ladder, we can also calculate the result without the $q \rightarrow 0$ ex-

pansion:

$$\Pi(q) = \sum_k \cos^2(qa/2) = \cos^2(qa/2). \quad (\text{S86})$$

Note that this means $\Pi(n) = 0$ for $|n| > 1$, exhibiting the compact localization properties of an exact flat band, visible in the behavior of G_0 . This however does not imply that the propagator V^{-1} is similarly localized.

Writing $z = T/T_c > 1$, the propagator is

$$\begin{aligned} V^{-1}(n) &= 4T \int_{-\pi/a}^{\pi/a} \frac{adq}{2\pi} \frac{e^{-iqna}}{z - \cos^2(qa/2)} \quad (\text{S87}) \\ &= \frac{4Te^{-|n|a/L_g}}{\sqrt{z(z-1)}}, \quad L_g = \frac{a}{\log[2z - 1 + 2\sqrt{z(z-1)}]}, \quad (\text{S88}) \end{aligned}$$

as found by changing variables $q = ia \ln z$ and calculating the residue.

The interaction-mediated supercurrent in the Creutz ladder is then

$$I_{c,\text{int}} = \frac{\Delta_L \Delta_R}{2T} \sqrt{z(z-1)} e^{-L/L_g}, \quad (\text{S89})$$

within the Ginzburg-Landau expansion and assuming $\mu = -2t$, $|t| \gg T$.

Comparison of the above to numerical calculations without the Ginzburg-Landau approximation are shown in Fig. S2. It assumes that Δ_n is fixed to $\Delta_S e^{-i\varphi/2}$ for $n \leq 0$, $\Delta_S e^{i\varphi/2}$ for $n \geq L/a$, and $\Delta_n = U \langle c_{n\uparrow} c_{n\downarrow} \rangle$ for $0 < n < L/a$ are determined self-consistently.

Computer codes

Computer codes used in this manuscript and the supplement can be found at <https://gitlab.jyu.fi/jyucmt/2024-flatband-s-junctions>.